Toward Standardized and Comparable Reporting for Sacrificial Photocatalytic Hydrogen Evolution

ACS Energy LETTERS

Open Access

http://pubs.acs.org/journal/aelccp

Perspective

Toward Standardized and Comparable Reporting for Sacrificial Photocatalytic Hydrogen Evolution

Alexandre Holmes* and Ergang Wang*

Cite This: *ACS Energy Lett.* 2026, 11, 4220−4229

Read Online

ACCESS | Metrics & More | Article Recommendations | Supporting Information

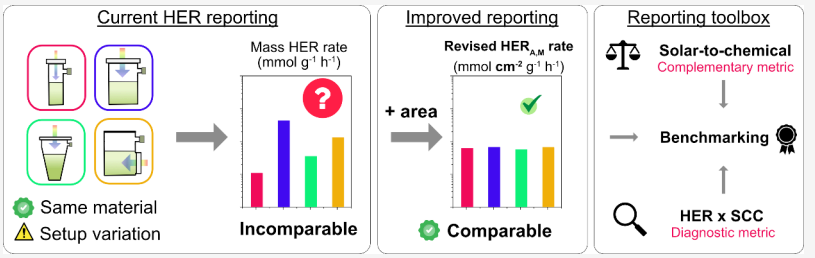

ABSTRACT: Sacrificial photocatalytic hydrogen evolution has advanced rapidly, yet meaningful benchmarking remains hindered by inconsistent metrics and the incomplete reporting of key experimental parameters. In this Perspective, we outline a minimal "reporting set"—intended to be practical for authors, reviewers, and editors—that improves transparency and enables cross-study comparison. We further show that the widely used mass-normalized hydrogen evolution rate (HER) can be strongly affected by the experimental conditions. As a simple step toward improved comparability, we advocate incorporating the irradiation surface area into rate reporting and introduce an area−mass normalized metric ($HER_{A,M}$), which markedly improves cross-study consistency. In addition, we explored solar-to-chemical conversion $SCC_{(H2)}$ as a complementary metric tailored for sacrificial hydrogen evolution and a diagnostic tool "HER × SCC" to identify trade-offs associated with photocatalyst concentrations. Finally, we propose a two-axis benchmarking concept ($HER_{A,M}$ and $SCC_{(H2)}$) to visualize performance and report quality simultaneously.

Hydrogen is widely recognized as a clean and versatile energy carrier, yet its current production is predominantly reliant on fossil fuels, resulting in substantial CO_2 emissions and undermining its environmental benefits.[1] Water electrolysis offers a greener route, particularly when powered by renewable electricity, but the high capital and operational costs continue to hinder large-scale adoption.[2] Photocatalytic hydrogen evolution represents a promising alternative, enabling solar-driven water splitting at potentially lower costs and a minimal carbon footprint. In addition, photocatalysis abstracts from the need of applied bias, required in photo electrocatalysis, and ensures a faster positive energetical balance.[3] However, the performance of state-of-the-art photocatalysts remains far below the U.S. Department of Energy (DOE) target for commercialization, which requires a solar-to-hydrogen (STH) conversion efficiency of 5−10% for dual bed photocatalyst hydrogen production.[4]

Typically, photocatalysts are dispersed in water in the form of nano- or microparticles, offering a scalable and low-cost approach that requires minimal infrastructure.[5,6] Despite its promise, overall water splitting (OWS) represents a challenge for most photocatalysts. Instead, hydrogen evolution reaction (HER) allows for partial water splitting through the addition of a sacrificial electron donor (SED) to overcome the intrinsic difficulty of the water oxidation.[7] This stimulated intense research efforts reflected on the research output of the past decade (Figure 1a).[8−11] In practice, sacrificial hydrogen generation remains costly and ineffective as SED is consumed along the process. In addition, to be a technology ready for large scale implementation, photocatalyst stability and operational lifetime must be further investigated.[12] Nevertheless, recent alternatives opened new avenues to a sustainable hydrogen production, replacing SED consumption by biomass valorization or pollutant degradation.[13−16]

However, a central challenge for sacrificial photocatalytic HER is the lack of standardized and comprehensive performance metrics.[17−22] The mass-normalized hydrogen evolution reaction rate (HER rate, mmol g^{-1} h^{-1})—currently the most widely reported benchmark—fails to adequately capture the overall performance. For instance, experimental parameters such as light intensity and sample irradiation area can largely influence the HER rate while not being considered. In addition, the mass-normalization strongly amplifies the influence of photocatalyst concentration, where highly diluted dispersions can lead to artificially inflated HER rates.[23] Nevertheless,

Received: February 19, 2026
Revised: March 30, 2026
Accepted: April 3, 2026
Published: May 1, 2026

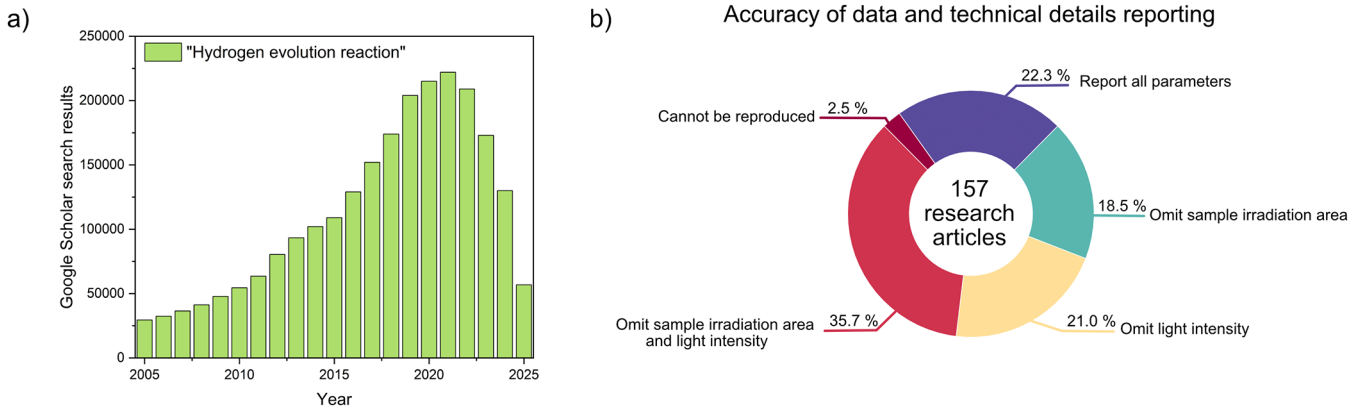

Figure 1. (a) Indicative Google Scholar search results "hydrogen evolution reaction" filtered for individual years. (b) Statistical analysis of 157 research articles published over the last 5 years in the field of hydrogen evolution reaction with common misconduct in reporting data and technical details (Supplementary Table S1). The description "cannot be reproduced" is linked to more than 3 technical details missing, including mass of the sample, volume of dispersion, or both.

comparative studies of photocatalyst review articles often need to rely on the mass-normalized HER rate despite its limited accuracy.[10,24]

Therefore, proper quantification of sacrificial HER performance is required to ensure that the expansion of the field is fair and rigorous, accounting for all experimental parameters. Beyond improved reporting, the community would also benefit from complementary metrics that capture different aspects of performance—analogous to how STH has helped standardize evaluation in OWS. Finally, rather than relying on a single universal figure of merit, developing diagnostic tools that make concentration-dependent trade-offs explicit can help distinguish genuinely improved photocatalysts from artifacts of experimental design and enable more meaningful benchmarking across studies.

THE STATE-OF-THE-ART METRIC

We summarized the technical details of 157 articles published over the last 5 years focusing on sacrificial hydrogen evolution in the Supplementary Table S1. It is important to note that our intention is to provide an objective overview of common pitfalls and methodological differences across groups rather than to critique the strengths or weaknesses of each work.

As showcased in Figure 1b, less than 25% of the selected articles provided sufficient details to reproduce the photocatalytic experiments, regardless of the material class (including inorganic[25] or organic semiconductors,[26] hybrid,[27] covalent organic frameworks,[28] carbon nitride[29]). In addition, some technical details can be scattered across the main text, the Supporting Information, or figure captions, making fair evaluation of the experimental conditions both time-consuming and error prone.

While mass normalized HER rates are widely adopted in the literature, the metric lacks accuracy. In most systems, the addition of a cocatalyst, such as Pt, is required to ensure hydrogen production, yet their mass contribution is typically excluded in the total photocatalyst mass calculation. We strongly recommend that the cocatalyst mass should be incorporated into the total mass calculation. For instance, we recalculated the normalized HER rates using a combined "total-mass" of both photocatalysts and cocatalyst in Supplementary Table S1. As a result, the apparent benefits of high cocatalyst loading are diminished, discouraging the excessive use of precious metals solely to boost performance metric.

DEFINING PHOTOCATALYTIC CONDITIONS

Photocatalytic setups can adopt a variety of architectures, thanks to the simplicity of their core requirements. Therefore, this technology is quite attractive for many research groups as both commercial and handmade systems can be used to provide good quality results. In practice, it can be divided into three key components with a solar simulator, a photocatalytic reactor, and a detection system (Figure 2a).

The quantification of hydrogen production, *i.e.* the outcome of the reaction, is mostly conducted by gas chromatography (GC) in the presence of a thermal conductivity detector (TCD), but other alternatives using hydrogen sensors are also explored to reduce setup costs.[30] Since GC is typically calibrated with standard H_2, the accuracy of this method is not a concern, considering that calibrations are up to date and checked periodically. The light sources, however, vary widely from LED-sources to Xenon light bulbs, which directly impact the light range (full arc, visible light only, AM 1.5G, etc.) and light intensity (varies from about 50 to over 300 mW cm^{-2}) used in the experiments.[35−39]

Moreover, we identified that variations in reactor design—particularly in reactor size and shape as well as light illumination direction, represent the main sources of discrepancy across research groups (Figure 2b). These design differences ultimately constrain key experimental parameters: dispersion volume (1 to 100 mL), mass of photocatalyst (0.1 to 50 mg), and reactor window area, *i.e.* sample irradiation area (from about 1 to over 30 cm^2), which have a significant impact on the HER rate and render results incomparable across different studies.[40−42] Other experimental details such as the temperature, pressure, pH, use of cosolvent, cocatalyst, or different SED can be modulated to tune HER performances yet are less likely to be limited by instrumentation and not covered in this discussion.[43−45]

Our overarching goal is to ensure reproducibility and clarity of the HER performance, allowing a fair comparison of performance across the literature and simplified benchmarking. The first step is the establishment of a minimal "reporting set", that allows for a transparent description of all the key-parameters involved in the HER experiment (available in Supplementary Note 1).

https://doi.org/10.1021/acsenergylett.6c00531
ACS Energy Lett. 2026, 11, 4220−4229

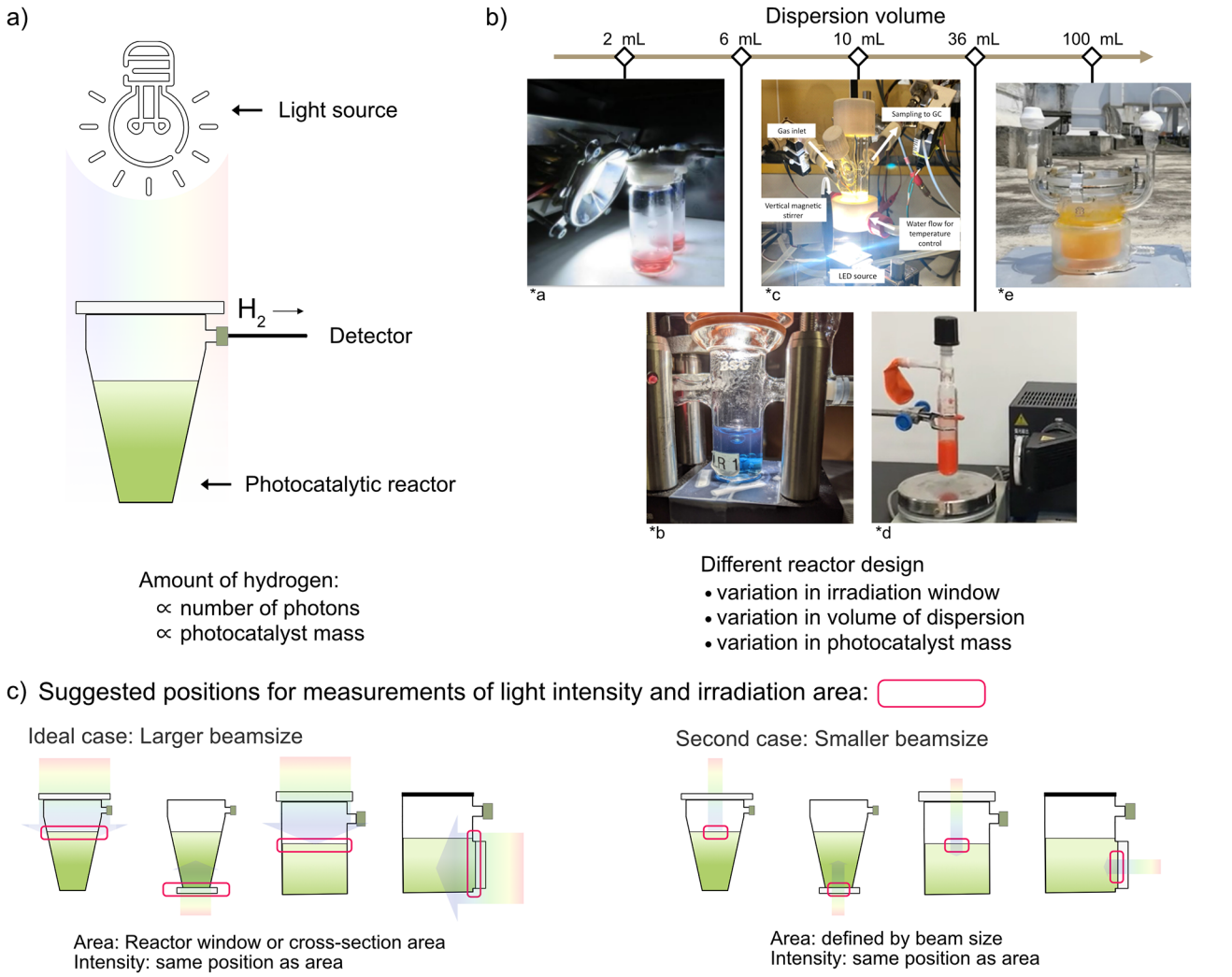

Figure 2. a) Schematic representations of the requirements for photocatalytic hydrogen evolution experiments and considerations that impact the hydrogen evolution. b) Representation of variability in reactor design and size, reproduced with permission from references *a,[30] *b,[31] *c,[32] *d,[33] and *e.[34] c) Schematic representation of light irradiation area and intensity measurement.

For clarity, we reinforce the focus on the parameters usually missing from current reports:

- The irradiation area, defined as the surface area of the photocatalyst that is exposed to the incident light. Suggested position for determining irradiation area depending on the reactor geometry is schematized in Figure 2c but is ideally measured at the surface of the photocatalyst which is exposed to the light source.
- The light intensity should be measured using a calibrated detector (*i.e.* photodiode, power meter, or reference cell) at the same position used for determining the irradiation area. For Xenon-light sources, the irradiation range (full arc or visible range) and filter conditions (such as AM 1.5G) should be mentioned clearly, as it directly impacts photon flux. In the case of LED light sources, the emission profile would strongly benefit reproducibility and transparency. For high performance benchmark reporting, we recommend relying on AAA solar simulator.

IMPACT OF SETUP VARIATIONS ON HER RATES

After defining the key parameters that should be reported in HER experiments, we conducted a series of photocatalytic experiments designed to mimic the range of reactors and reporting variations commonly encountered in the literature. To simplify HER experiments, we selected $PF_gBTSO\text{-}T_{25}$ as the photocatalyst without photodeposition of a metallic cocatalyst, thereby minimizing the influence of varying conditions on cocatalyst formation and subsequent efficiency.[44,46] Table 1 summarizes the experimental parameter matrix (photocatalyst mass, irradiation window area, dispersion volume, and photocatalyst concentration) and the resulting HER rates expressed using different normalization schemes, including non-normalized rates as well as mass-, area-, and volume-based metrics.

As expected, even for the same photocatalysts, the HER rates vary substantially across experimental conditions (Figure 3a). Importantly, these controlled variations provide a direct way to identify which experimental parameters most strongly bias commonly reported metrics and, in turn, which normalizations most effectively improve comparability across studies.

We can first examine the effect of photocatalyst mass, or concentration, on the amount of hydrogen produced. At first, increasing the photocatalyst loading enhances the non-normalized HER rate, due to a greater number of active sites (that we define as linear regime). However, beyond a certain threshold the rate plateaus are likely due to shielding effects

https://doi.org/10.1021/acsenergylett.6c00531
ACS Energy Lett. 2026, 11, 4220−4229

Table 1. Experimental Parameters Used for Photocatalytic Experiments from the $PF_gBTSO\text{-}T_{25}$ Dispersion and Corresponding HER Rates Expressed Using Different Normalization Metric Systems[d]

	Setup variations					Normalized HER rate by							
Entry	Mass (mg)	Concentration (μg mL^{-1})	Irradiation area (cm^2)	Volume (mL)	Non-normalized HER rate (μmol h^{-1})	Volume and mass (mmol g^{-1} h^{-1} L^{-1})	Volume (mmol h^{-1} L^{-1})	Conc.[a] (mmol L g^{-1} h^{-1})	Mass (mmol g^{-1} h^{-1})	Area (mmol cm^{-2} h^{-1})	Volume and area (mmol cm^{-2} h^{-1} L^{-1})	Conc.[a] and area (mmol L cm^{-2} g^{-1} h^{-1})	Mass and area (mmol cm^{-2} g^{-1} h^{-1})
1	**0.25**	**8.3**	10	30	60	8000	2.00	7.20	240	0.006	0.20	0.72	24.0
2	**0.5**	**16.7**	10	30	81	5400	2.70	4.86	162	0.008	0.27	0.49	16.2
3	**0.75**	**25**	10	30	140	6222	4.67	5.60	187	0.014	0.47	0.56	18.7
4	**1.0**	**33,3**	10	30	203	6767	6.77	6.09	203	0.020	0.68	0.61	20.3
5[b]	**1.5**	**50**	10	30	158	3511	5.27	3.16	105	0.016	0.53	0.32	10.5
6	0.75	25	**4**	30	59	2622	1.97	2.36	79	0.015	0.49	0.59	19.7
7	0.75	25	**2.9**	30	47	2089	1.57	1.88	63	0.016	0.54	0.65	21.6
8	0.75	25	**1.4**	30	26	1156	0.87	1.04	35	0.019	0.62	0.74	24.8
9	0.25	25	10	**10**	41	16400	4.10	1.64	164	0.004	0.41	0.16	16.4
10	**0.5**	**16,7**	**4**	**30**	43	2867	1.43	2.58	86	0.011	0.36	0.65	21.5
Average	-	-	-	-	86	5503	3.13	3.64	132	0.013	0.46	0.55	19.4
Std. Dev.	-	-	-	-	60	4433	1.95	2.13	68	0.005	0.15	0.18	4.2
CV	-	-	-	-	**0.70 / 0.73** [c]	**0.81 / 0.81** [c]	**0.62 / 0.66** [c]	**0.59 / 0.61** [c]	**0.51 / 0.53** [c]	**0.42 / 0.45** [c]	**0.33 / 0.35** [c]	**0.33 / 0.30** [c]	**0.22 / 0.15** [c]

[a]Corresponds to the concentration of photocatalysts in the dispersion. [b]Reflects the impact of concentration toward reproducibility, outside of the linear regime described in Figure 3a. [c]Corresponds to the CV calculated only considering linear regimes of concentrations (excluding entry 5). [d]The average, standard deviation, and coefficient of variability were calculated based on ten experimental conditions. All experiments were conducted over 5 h in the presence of ascorbic acid (0.1 M), under full-arc Xe irradiation using an AM 1.5G filter (100 mW cm^{-2}), with reduced pressure (1.2 kPa) at room temperature.

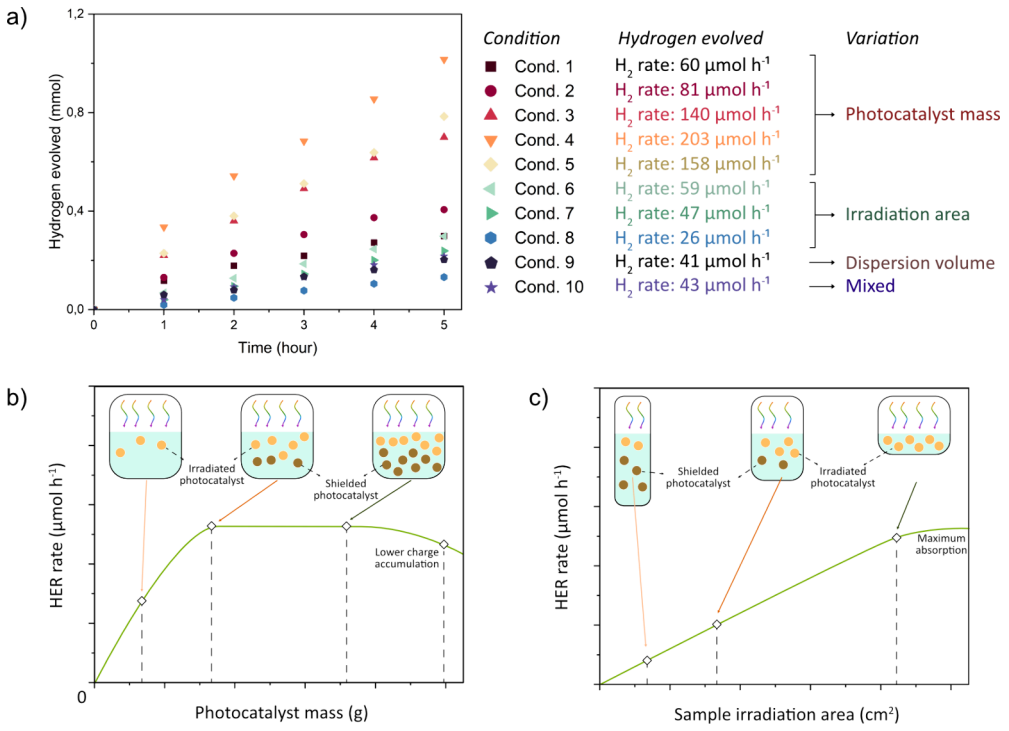

Figure 3. a) Non-normalized hydrogen evolution using different experimental conditions, as detailed in Table 1. Non-normalized HER rates presented were calculated after 5 h of experiment. b) Schematic representation of the hydrogen evolution rate as a function of the mass of photocatalysts while keeping constant the volume and irradiation surface. c) Schematic representation of the hydrogen evolution rate as a function of the sample irradiation area, i.e., reactor window, while keeping constant the mass of photocatalyst and volume.

(Figure 3b), defining a saturation regime.[18] Eventually, we can observe a decrease in the HER rate with a further increase of photocatalyst mass (entry 5). Such behavior can be explained either by excessive light scattering[47] or reduced charge accumulation per particle[37,41] but is not linked to setup limitations.

Therefore, it is important to understand the impact of photocatalyst concentration to promote the use of photocatalysts in the linear regime, ensuring reproducibility and comparability. This is especially true when mass-normalized metrics are used. To this extent, we strongly recommend performing concentration dependent HER experiments, which are present in the "reporting set" (Supplementary Note 1). Such experiments would showcase that performances are obtained in appropriate concentration regime.

https://doi.org/10.1021/acsenergylett.6c00531
ACS Energy Lett. 2026, 11, 4220−4229

When considering the irradiation window area, *i.e.* the sample irradiation surface, a linear trend can be observed (Figure 3c). We anticipate that a plateau could also be reached once the light absorption of the photocatalyst reaches saturation. Finally, the dispersion volume appeared to slightly affect the HER rates. When comparing entries 1 and 9, which have the same photocatalyst mass but different volumes, a decrease in volume resulted in a decrease of the HER rates by about 30%. This trend is consistent with the larger volume (lower effective concentration), reducing optical shielding/scattering and improving light penetration through the suspension.

Given the substantial discrepancies observed across experimental conditions, it becomes essential to quantify this variability and identify appropriate normalization strategies. The variance (or standard deviation, St. dev.) is typically used to assess data reproducibility but requires consistent units across data sets. To enable cross-comparison, we therefore calculated the coefficient of variation (CV) for all HER rates, which provides a unit-independent measure of relative variability, as defined in eqs 1 to 3

$$Average = \frac{\Sigma^N X}{N} \tag{1}$$

$$St.\ dev. = \sqrt{\frac{\Sigma^N (X - average)^2}{N}} \tag{2}$$

$$\mathrm{CV} = \frac{St.\ dev.}{Average} \tag{3}$$

where X corresponds to the calculated HER rate from each individual entry, and N corresponds to the data set size (here $N = 10$). A larger CV corresponds to greater variability and poorer reproducibility across measurements, while a smaller CV reflects more consistent and reliable data. From the non-normalized HER rates, we calculated a CV of 0.70, highlighting substantial variability across the experiments (Table 1). To improve the comparability across experiments, we selected several parameters with the objective of providing direct representativity in terms of practical application: size of the final photocatalytic cell (irradiation area of the sample, volume of the dispersion) and amount of photocatalyst (mass). We excluded the light's penetration depth as this parameter will be linked to photocatalysts' absorption coefficient and concentration.

The mass normalized HER rate (mmol g^{-1} h^{-1}) allowed a decrease in the CV value to 0.51 but remained relatively high. Considering the large impact of sample irradiation area on the HER rate, it is natural to consider an area normalized HER rate (mmol cm^{-2} h^{-1}), leading to a further reduced CV of 0.42. However, normalization based on the volume of dispersion (mmol L^{-1}) or concentration of photocatalysts (mmol L g^{-1}) remained inconclusive with a high CV.

We next investigated the effect of combining two parameters to further decrease the CV within the different photocatalytic experiments (Table 1). By combination of the sample irradiation area to either the volume or the concentration of photocatalysts, the CV could be reduced by around 0.33. Yet the best alternative appeared to be the combination of sample irradiation area and mass of photocatalyst (identified as $HER_{A,M}$ in mmol cm^{-2} g^{-1} h^{-1}), with a minimum CV value of 0.22 achieved, quite in agreement with the main parameters previously identified as most influential on HER rates (Figures 3b, 3c).

Such a straightforward adjustment can allow a more representative assessment of photocatalytic performance, and the transition from the conventional mass normalized HER rate to this dual normalization is both practical and easily implemented. In addition, adopting this revised metric also introduces a necessary benchmarking requirement: explicit reporting of the reactor window or irradiation area (depending on whether the beam fully covers the reactor surface). Yet this information is frequently absent from the literature—among the 157 selected articles, less than half reported the reactor irradiation area used (Supplementary Table S1). Standardizing such reporting practices would therefore represent a critical step toward fairer and more reproducible comparisons of the photocatalyst performance.

An analysis of 157 published articles shows that less than 25% report sufficient experimental details to ensure reproducibility, with light intensity or irradiation area often omitted.

Although the new metric with dual normalization (mass and area) can reduce the discrepancy between experimental setups, it still lacks the representativity of two parameters: the light intensity and the concentration of photocatalyst used during the photocatalytic experiments. In the following sections, we propose strategies to overcome these critical issues.

Combining mass- and surface-normalization improves reproducibility by more than a factor of two, while requiring readily accessible experimental parameters.

A METRIC FOR ENERGY CONVERSION

To fully understand the competitiveness of a photocatalyst, a metric that accounts for the energetical conversion happening during the photocatalytic experiment is crucial. In the field of photocatalytic water splitting, the solar-to-hydrogen (STH) conversion is defined as the ratio of energy stored as H_2 to the incident solar energy, as expressed in Equation 4

$$\mathrm{STH} = \frac{Output\ energy\ as\ H_2}{Input\ energy\ from\ solar\ light} = \frac{\Delta G_{OWS} \times r_{H2}}{P_{sun} \times S} \tag{4}$$

where ΔG_{OWS} is the reaction Gibbs energy of water splitting (J mol^{-1}), r_{H2} is the hydrogen evolution rate (mol s^{-1}), P_{sun} is the light intensity of the solar irradiation (mW cm^{-2}), and S is the irradiated area of the sample (cm^2), corresponding to the reactor window size.

By definition, STH is not directly applicable to HER reactions with the addition of SED, since the Gibbs free energy of water splitting (237 kJ mol^{-1}) exclusively represents true water splitting reaction.[18,48] Therefore, the contribution of SED to the

https://doi.org/10.1021/acsenergylett.6c00531
ACS Energy Lett. 2026, 11, 4220−4229

hydrogen evolution complicates the direct comparison between true OWS and HER with SED.[49]

> The field of HER lacks a practical metric for quantifying energy conversion, in contrast to established benchmarks such as the solar-to-hydrogen efficiency in water splitting.

To address this limitation, we explored the benefits of using solar-to-chemical conversion (SCC), defined in Equation 5 for other photocatalytic reactions. This metric has previously been used in the field of photocatalytic hydrogen peroxide production ($SCC_{(H2O2)}$)[50] and can be readily adapted for HER, following eq 6

$$SCC = \frac{Output\ energy\ as\ chemical}{Input\ energy\ from\ solar\ light} = \frac{\Delta G_r \times r_{chem}}{P_{sun} \times S} \quad (5)$$

$$SCC_{(H2)} = \frac{Output\ energy\ as\ hydrogen}{Input\ energy\ from\ solar\ light} = \frac{\Delta G_{HER} \times r_{H2}}{P_{sun} \times S} \quad (6)$$

where ΔG_r is the Gibbs free energy of the reaction, and r_{chem} is the rate of production of the chemical achieved in the photocatalytic reaction. When applied to the HER, ΔG_{HER} accounts for both the reduction of protons and the oxidation of SED and can be defined in Equation 7

$$\Delta G_{HER} = -n \times F \times E_{HER} \quad (7)$$

where n is the number of electrons involved in the reaction, F corresponds to the Faraday constant (96 485 C mol^{-1}), and E_{HER} is the reaction potential difference of SED oxidation and proton reduction (V) versus the standard hydrogen electrode (SHE). For example, we can select HER reactions performed in the presence of ascorbic acid (AA). Both half-reactions are developed in Equations 8 and 9, where DHA (dehydroascorbic acid) stands for the oxidized form of AA. The potential difference E_r can then be calculated as in Equation 10, followed by the Gibbs free energy representative of the hydrogen evolution reaction in the presence of AA in Equation 11.

$$2H^+ + 2e^- \leftrightarrow H_2 \quad (8)$$

$$DHA + 2H^+ + 2e^- \leftrightarrow AA \quad (9)$$

$$E_{HER}^{AA} = E_{red}^{H+/H2} - E_{red}^{DHA/AA} = -0.39\ V \quad (10)$$

$$\Delta G_{HER}^{AA} = -2 \times 96485 \times -0.39 = 75258\ J\ mol^{-1} \quad (11)$$

Therefore, $SCC_{(H2)}$ can be calculated by knowing the Gibbs free energy describing the HER reaction, the irradiation surface, and light intensity used during experiments. It provides a depiction of the practical amount of hydrogen produced in regards of the energy input. As it directly scales with light intensity, it enables additional insights toward intensity-dependence properties. In the previous example, AA was selected as the SED material, but $SCC_{(H2)}$ calculations can be further applied to other SEDs, as detailed in Supplementary Note 2. Therefore, it is important to establish the requirements for the $SCC_{(H2)}$ calculation:

i. The oxidation product(s) from the SED should be clearly identified. SEDs that can undergo multiple oxidation pathways (e.g., methanol, lactic acid) cannot be selected for $SCC_{(H2)}$ by using a single redox potential. It becomes mandatory to identify the specific redox couple involved along all the process, to provide a more accurate descriptor of the thermodynamics behind HER reaction.
ii. $SCC_{(H2)}$ should only be applied when both redox half-reactions are energetically uphill and nonspontaneous ($\Delta G_r > 0$), ensuring that the hydrogen production is only a product of photocatalysis.

Nevertheless, $SCC_{(H2)}$ remains sensitive to variations in light source characteristics and photon flux. Apparent quantum yield (AQY) or quantum efficiency (QE), determined under monochromatic light, provides additional benchmarks less sensitive to photon flux. However, accurate determination of photon flux requires explicit reporting of the measurement protocol, including the type of detector, spectral range, calibration procedure, and measurement position relative to the photocatalyst. It should be noted that to ensure meaningful comparison, experimental conditions between AQY and HER measurements should remain consistent with the light source as the primary variable. For instance, the photocatalyst concentration can strongly affect AQY performance. In addition, charge

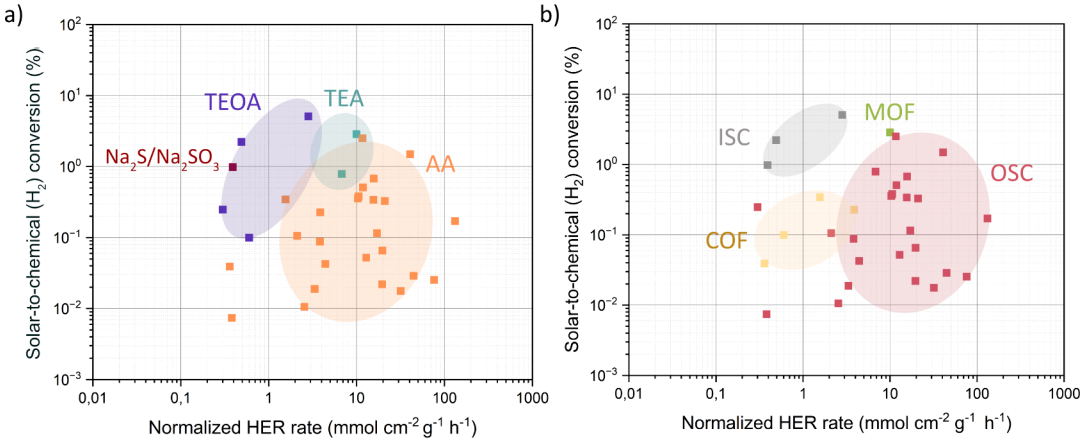

Figure 4. Ashby plot of $HER_{A,M}$ and $SCC_{(H2)}$ as a function of a) the type of SED material and b) the photocatalyst type. Abbreviations used stand for triethylamine (TEA), triethanolamine (TEOA), inorganic semiconductors (ISC), organic semiconductors (OSC), covalent organic framework (COF), and metallic organic framework (MOF).

https://doi.org/10.1021/acsenergylett.6c00531
ACS Energy Lett. 2026, 11, 4220−4229

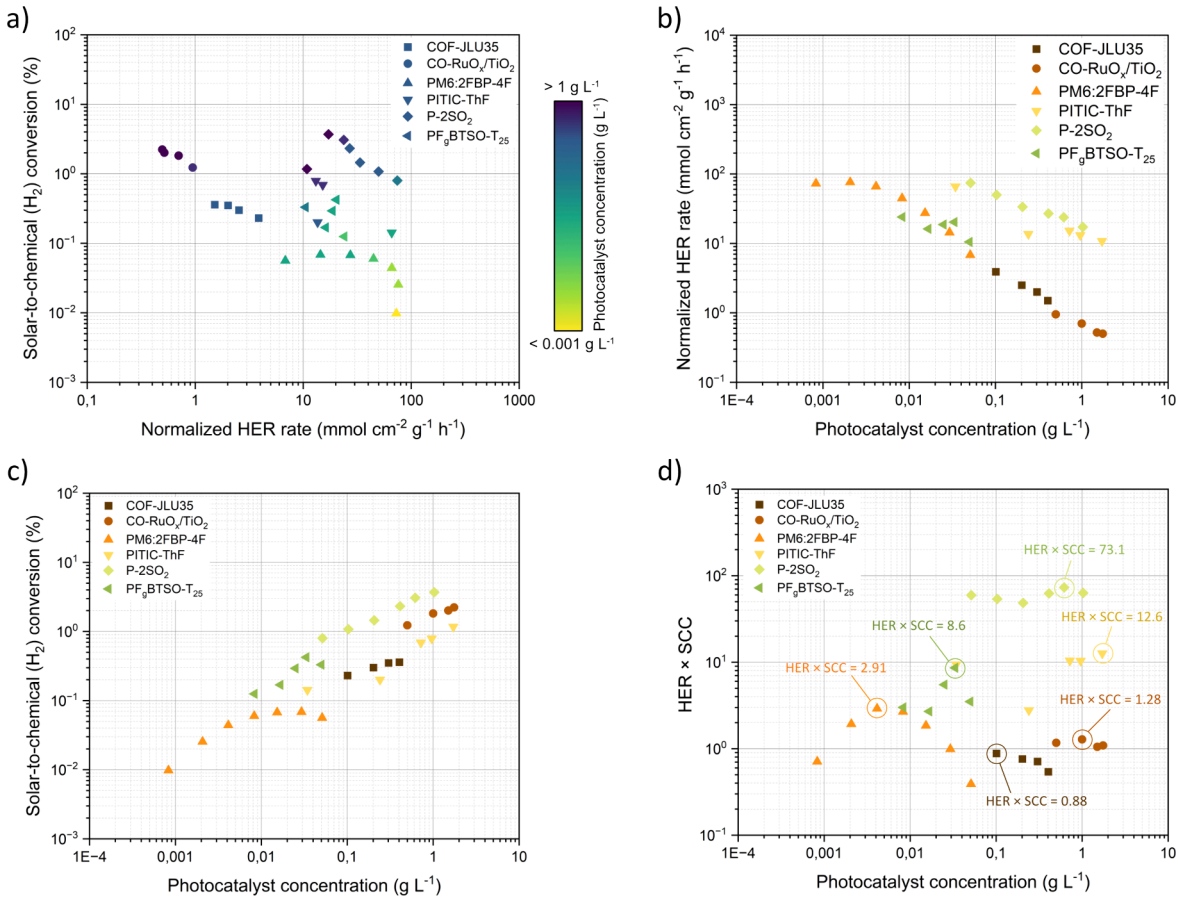

Figure 5. a) Ashby plot representing $SCC_{(H2)}$ as a function of $HER_{A,M}$ rates following the impact of different photocatalyst concentrations and identification of the optimum concentration with the HER × SCC highlighted. Impact of the photocatalyst concentration on b) normalized $HER_{A,M}$ rate, c) $SCC_{(H2)}$, and d) HER × SCC. In addition to the data collected in this work ($PF_gBTSO\text{-}T_{25}$), other systems were reported elsewhere: COF-JLU35,[53] CO-RuO_x/TiO_2,[25] PM6:2FBP-4F,[41] PITIC-ThF,[36] and P-$2SO_2$.[54]

generation and accumulation under monochromatic light measurements are incomparable to full-spectrum conditions, since significantly lower light intensities are usually used, potentially overestimating the actual performance of the photocatalyst under practical illumination.[51]

VERSATILE DATA DISPLAY AND COMPARABILITY

Building on the previous section, combining the normalized $HER_{A,M}$ rate and $SCC_{(H2)}$ through an Ashby plot provides a more comprehensive understanding of photocatalyst performance (Figure 4): the former compares the intrinsic performance across photocatalysts, while the latter quantifies practical conversion rates for a defined incident solar energy input. Owing to insufficient technical details, only 36 of the 157 initially selected research articles provided sufficient information for the calculation of $SCC_{(H2)}$ (Supplementary Table S2).

As a benchmarking concept, we showcase how the impact of SED material (Figure 4a) and photocatalyst type (Figure 4b) could be emphasized using a two axis plot of $HER_{A,M}$ and $SCC_{(H2)}$. While the number of data points remained limited, this first data set can be used to exemplify the benefits for future research: trends can be identified among the type of SED or photocatalyst, with, for instance, the combination of AA and OSC usually yielding high $HER_{A,M}$ while moderate $SCC_{(H2)}$. Such a combination of both metrics provides additional insights, usually limited to $HER_{A,M}$ rates comparison.[52] We encourage the community to actively complement and enrich this plot to facilitate identification of the most promising candidates. Ultimately, this concept can improve comparability across systems and setups while providing versatile data display that can be used to emphasize stability, absorption range, cost, toxicity, etc.

A DIAGNOSTIC METRIC HER × SCC

When it comes to practical applications, the photocatalyst concentration directly impacts the overall size of the reactor. For instance, using 1 g of photocatalyst at the concentration of 1 g L^{-1} or at 1 mg L^{-1} will require reactor volumes differing by a factor of 1000. Therefore, while high mass normalized HER rates are desired, the concentration of the photocatalyst should remain reasonably high for practical applications. Conversely, higher concentrations typically yield higher $SCC_{(H2)}$ values due to greater total hydrogen production. This reflects a fundamental trade-off in photocatalysis driven by changes in photocatalyst concentrations. The identification of the best concentration to use when considering only $HER_{A,M}$ or $SCC_{(H2)}$ might become challenging, as displayed in Figure 5a. In addition, the identification of the operational regime (linear or saturation) is required to understand whether photocatalysts are in their optimum concentration range. To reconcile these opposing effects and achieve a balanced assessment, we introduce a combined concept, "HER × SCC". This metric functions as a diagnostic tool that captures the interplay between photocatalyst

https://doi.org/10.1021/acsenergylett.6c00531
ACS Energy Lett. 2026, 11, 4220−4229

activity and solar energy utilization, identifying the optimum concentration regime where both are maximized.

We analyzed five research articles that reported different photocatalyst concentrations, in addition to our own experiments, to investigate the benefits of HER × SCC (Supplementary Table S3). First, we could identify that the normalized $HER_{A,M}$ rate is increased by lowering the concentration of the photocatalyst (Figure 5b), which is consistent with reduced light scattering and enhanced photon penetration. In contrast, $SCC_{(H2)}$ decreases with lower concentration (Figure 5c) due to smaller overall hydrogen yields under diluted conditions.

Our results demonstrate that HER × SCC provides a balanced measure of performance without inherently favoring either high or low photocatalyst concentrations. As exemplified in Figure 5d, the maximum HER × SCC value simplifies the identification of optimum concentration ranges. In practice, the higher the value, the more competitive the photocatalyst, but its use should not be directed toward a single digit figure of merit, rather complement additional discussion and experimental validations. To the best of our knowledge, this constitutes the first diagnostic tool for concentration trade-offs proposed in the field of photocatalysis, despite its critical importance for consistent benchmarking and the advancement of the field.

Diagnostic metrics such as HER × SCC enable a meaningful assessment of photocatalytic performances, avoiding artificial inflation of mass-normalized HER rates at extreme dilution factors.

Through this Perspective, we aim to develop a transparent and multidimensional framework for the evaluation of photocatalytic performance. Reporting photocatalytic performance would be simplified by following guidelines, such as those proposed in the "reporting set". Furthermore, we highlight that a dual area- and mass-normalization largely improves reproducibility and comparability of $HER_{A,M}$ rates, mitigating the impact of setup geometry and allowing for fair comparison of photocatalyst performance across research institutes. The solar-to-chemical conversion ($SCC_{(H2)}$) acts as a complementary metric, accounting for the impact of the light intensity and SED material. Through the development of complementary metrics, a "reporting toolbox" can emerge, providing a more complete overview of photocatalysts performance. Finally, we propose a two-axis mapping ($HER_{A,M}$ and $SCC_{(H2)}$) as a benchmark concept to simplify comparison across different experiments, an aspect that has long been challenging.

Standardizing HER reporting and relying on comparable and complementary metrics will improve how the field communicates progress while strengthening credibility. By accelerating the identification of "truly" high-performing materials, we will facilitate streamlining the pathway from small-scale experiments to pilot-scale validation will be facilitated. As the urgency for clean hydrogen intensifies, establishing rigorous and transparent performance reporting is not merely a technical improvement; it is a prerequisite for translating photocatalytic hydrogen production from a promising concept into a viable contributor to the global energy transition.

■ ASSOCIATED CONTENT

Supporting Information

The Supporting Information is available free of charge at https://pubs.acs.org/doi/10.1021/acsenergylett.6c00531.

Materials and Methods, Supplementary Tables, Supplementary Notes 1 and 2, and references (PDF)

■ AUTHOR INFORMATION

Corresponding Authors

Alexandre Holmes − *Department of Chemistry and Chemical Engineering, Chalmers University of Technology, Göteborg SE-412 96, Sweden;* orcid.org/0009-0003-1340-4602; Email: holmesal@chalmers.se

Ergang Wang − *Department of Chemistry and Chemical Engineering, Chalmers University of Technology, Göteborg SE-412 96, Sweden;* orcid.org/0000-0002-4942-3771; Email: ergang@chalmers.se

Complete contact information is available at: https://pubs.acs.org/10.1021/acsenergylett.6c00531

Notes

The authors declare no competing financial interest.

Biographies

Alexandre Holmes is a Post-Doctoral researcher at Chalmers University of Technology (Gothenburg, Sweden). He received his Ph.D. in Polymer Chemistry in 2023 from the University of Pau and Pays de l'Adour (Pau, France). His research focuses on synthesis and formulation of aqueous organic semiconductor dispersions for water-processed electronics and photocatalytic reactions.

Ergang Wang is a Professor of Polymer Chemistry at Chalmers University of Technology (Gothenburg, Sweden). His research spans organic and hybrid semiconductors for solar-energy conversion, including photocatalytic hydrogen evolution and organic photovoltaics, as well as conjugated polymers for organic electronics, spanning materials design, photophysics, and device/system-level characterization (https://www.chalmers.se/en/persons/ergang/).

■ ACKNOWLEDGMENTS

We acknowledge the Swedish Research Council (2020-05223), the Swedish Research Council Formas (2023-01008), the Swedish Energy Agency (P2021-90067), the Wallenberg Foundation (2022.0192), and the Chalmers Area of Advances Energy and Nano for financial support.

■ REFERENCES

(1) IEA. *The Future of Hydrogen*. (2019).

(2) Serik, A.; Kuspanov, Z.; Daulbayev, C. Cost-effective strategies and technologies for green hydrogen production. *Renew. Sustain. Energy Rev.* **2026**, *226*, 116242.

(3) Tam, B.; Babacan, O.; Kafizas, A.; Nelson, J. Comparing the net-energy balance of standalone photovoltaic-coupled electrolysis and photoelectrochemical hydrogen production. *Energy Environ. Sci.* **2024**, *17*, 1677−1694.

(4) *DOE Technical Targets for Hydrogen Production from Photoelectrochemical Water Splitting*, Https://Www.Energy.Gov/Eere/Fuelcells/Doe-Technical-Targets-Hydrogen-Production-Photoelectrochemical-Water-Splitting, (Accessed 10 October 2025).

(5) Kim, J. H.; Hansora, D.; Sharma, P.; Jang, J.-W.; Lee, J. S. Toward practical solar hydrogen production − an artificial photosynthetic leaf-to-farm challenge. *Chem. Soc. Rev.* **2019**, *48*, 1908−1971.

(6) Pinaud, B. A.; et al. Technical and economic feasibility of centralized facilities for solar hydrogen production via photocatalysis and photoelectrochemistry. *Energy Environ. Sci.* **2013**, *6*, 1983.
(7) Wang, Y.; et al. Current understanding and challenges of solar-driven hydrogen generation using polymeric photocatalysts. *Nat. Energy* **2019**, *4*, 746−760.
(8) Lyons, R. J.; Sprick, R. S. Processing polymer photocatalysts for photocatalytic hydrogen evolution. *Mater. Horiz.* **2024**, *11*, 3764−3791.
(9) Holmes, N. P.; et al. Organic semiconductor colloids: From the knowledge acquired in photovoltaics to the generation of solar hydrogen fuel. *Curr. Opin. Colloid Interface Sci.* **2021**, *56*, 101511.
(10) Ullah, I.; Amin, M.; Zhao, P.; Qin, N.; Xu, A.-W. Recent advances in inorganic oxide semiconductor-based S-scheme heterojunctions for photocatalytic hydrogen evolution. *Inorg. Chem. Front.* **2025**, *12*, 1329−1348.
(11) Zhou, J.; Tian, Y.; Gu, H.; Jiang, B. Photocatalytic hydrogen evolution: Recent advances in materials, modifications, and photothermal synergy. *Int. J. Hydrog. Energy* **2025**, *115*, 113−130.
(12) Sivula, K. Are Organic Semiconductors Viable for Robust, High-Efficiency Artificial Photosynthesis? *ACS Energy Lett.* **2020**, *5*, 1970−1973.
(13) Yan, Q.; et al. Rational Design of Advanced Functional Catalysts for Photo-Reforming Glucose into Bio-Derived Fuels and Chemicals. *Adv. Sci.* **2025**, *12*, e08850.
(14) Niu, F.; et al. State-of-the-art and perspectives of hydrogen generation from waste plastics. *Chem. Soc. Rev.* **2025**, *54*, 4948−4972.
(15) Ya, Z.; Zhang, S.; Xu, D.; Wang, H.; Li, M. Coupling Plastic Upgrading and Photocatalysis: Catalytic Mechanisms and Design Principles. *ACS Catal.* **2025**, *15*, 5339−5369.
(16) Han, B.; et al. Synergistic hydrogen production and organic pollutant removal via dual-functional photocatalytic systems. *J. Environ. Sci.* **2025**, *153*, 202.
(17) Qureshi, M.; Takanabe, K. Insights on Measuring and Reporting Heterogeneous Photocatalysis: Efficiency Definitions and Setup Examples. *Chem. Mater.* **2017**, *29*, 158−167.
(18) Wang, Z.; et al. Efficiency Accreditation and Testing Protocols for Particulate Photocatalysts toward Solar Fuel Production. *Joule* **2021**, *5*, 344−359.
(19) Cao, S.; Piao, L. Considerations for a More Accurate Evaluation Method for Photocatalytic Water Splitting. *Angew. Chem., Int. Ed.* **2020**, *59*, 18312−18320.
(20) Melchionna, M.; Fornasiero, P. Updates on the Roadmap for Photocatalysis. *ACS Catal.* **2020**, *10*, 5493−5501.
(21) Sayago-Carro, R.; Jiménez-Chavarriga, L. J.; Fernández-García, E.; Kubacka, A.; Fernández-García, M. Efficiency in photocatalytic production of hydrogen: energetic and sustainability implications. *Energy Adv.* **2024**, *3*, 2738−2757.
(22) Kunz, L. Y.; et al. Artificial inflation of apparent photocatalytic activity induced by catalyst-mass-normalization and a method to fairly compare heterojunction systems. *Energy Environ. Sci.* **2019**, *12*, 1657−1667.
(23) Kisch, H.; Bahnemann, D. Best Practice in Photocatalysis: Comparing Rates or Apparent Quantum Yields? *J. Phys. Chem. Lett.* **2015**, *6*, 1907−1910.
(24) Murugan, P.; Liu, S.-Y. Innovative approaches to the molecular design, synthesis, and functionalization of conjugated organic polymer (D−A, D−π−A, A−A−D, and A−D−A) photocatalysts for sustainable hydrogen production. *J. Mater. Chem. A* **2025**, *13*, 30870.
(25) Shen, J.; et al. Single-Atom Co-Ultrafine RuO_x Clusters Codecorated TiO_2 Nanosheets Promote Photocatalytic Hydrogen Evolution: Modulating Charge Migration, H^+ Adsorption, and H_2 Desorption of Active Sites. *Adv. Funct. Mater.* **2024**, *34*, 2309056.
(26) Kosco, J.; et al. Generation of long-lived charges in organic semiconductor heterojunction nanoparticles for efficient photocatalytic hydrogen evolution. *Nat. Energy* **2022**, *7*, 340−351.
(27) Zhang, B.; et al. Facile Synthesis of Organic−Inorganic Hybrid Heterojunctions of Glycolated Conjugated Polymer-TiO_{2-X} for Efficient Photocatalytic Hydrogen Evolution. *Small* **2024**, *20*, 2402649.
(28) Zhao, W.; et al. Nanoscale covalent organic frameworks for enhanced photocatalytic hydrogen production. *Nat. Commun.* **2024**, *15*, 6482.
(29) Zeng, H.; et al. Interfacial Engineering of TiO_2 /Ti_3C_2 MXene/Carbon Nitride Hybrids Boosting Charge Transfer for Efficient Photocatalytic Hydrogen Evolution. *Adv. Energy Mater.* **2022**, *12*, 2102765.
(30) Bruder, J.; et al. Photocatalytic Hydrogen Generation in Surfactant-Free, Aqueous Organic Nanoparticle Dispersions. *Small* **2024**, *20*, 2406236.
(31) De La Perrelle, J. M.; et al. Red-Light-Mediated Photocatalytic Hydrogen Evolution by Hole Transfer from Non-Fullerene Acceptor Y6. *J. Phys. Chem. C* **2022**, *126*, 14518−14528.
(32) Larrieu, A.; Das, S. K.; Viterisi, A.; Billon, L. Self-Assembly-Induced Colloidal Covalent Organic Frameworks Toward Photocatalytic H_2 Evolution: A Surfactant-Free Concept. *Small* **2025**, *21*, 2505636.
(33) Tan, Z.-R.; et al. EDOT-based conjugated polymers accessed *via* C−H direct arylation for efficient photocatalytic hydrogen production. *Chem. Sci.* **2022**, *13*, 1725−1733.
(34) Liu, Y.; Wu, J.; Wang, F. Dibenzothiophene-S,S-dioxide-containing conjugated polymer with hydrogen evolution rate up to 147 mmol g−1 h−1. *Appl. Catal. B Environ.* **2022**, *307*, 121144.
(35) Pavliuk, M. V.; Wrede, S.; Tian, H. Phenoxazine-based small molecule heterojunction nanoparticles for photocatalytic hydrogen production. *Chem. Commun.* **2023**, *59*, 5611−5614.
(36) Elsayed, M. H.; et al. Overcoming small-bandgap charge recombination in visible and NIR-light-driven hydrogen evolution by engineering the polymer photocatalyst structure. *Nat. Commun.* **2024**, *15*, 707.
(37) Wu, S.; et al. Reversing Surface Charge for Highly-Active Organic Photovoltaic Catalysts. *Angew. Chem., Int. Ed.* **2025**, *64*, e202422779.
(38) Sun, H.; et al. A Carboxylate-based Hydrophilic Organic Photovoltaic Catalyst with a Large Molecular Dipole Moment for High-Performance Photocatalytic Hydrogen Evolution. *Angew. Chem., Int. Ed.* **2025**, *64*, e202503792.
(39) Wang, Y.; et al. Boosted Hydrogen Evolution via Photoinduced Hole Transfer in Molecular-Level Organic Heterojunction under NIR Photon Excitation. *Adv. Mater.* **2025**, *37*, 2415161.
(40) Brnovic, A.; Hammarström, L.; Tian, H. Mechanistic Insights into the Photocatalytic Hydrogen Production of Y5 and Y6 Nanoparticles. *J. Phys. Chem. C* **2023**, *127*, 12631−12639.
(41) Zhang, Z.; et al. Delocalizing Excitation for Highly-Active Organic Photovoltaic Catalysts. *Angew. Chem., Int. Ed.* **2024**, *63*, e202402343.
(42) Sheng, Q.; et al. The introduction of dual pyridinic N atoms into dibenzo[b,d]thiophene sulfone containing conjugated polymers for improved hydrogen evolution: Experimental and theoretical study. *Appl. Surf. Sci.* **2022**, *603*, 154425.
(43) Hao, L.; et al. Boosting exciton dissociation and charge separation in pyrene-based linear conjugated polymers for efficient photocatalytic hydrogen production. *J. Mater. Chem. A* **2022**, *10*, 24064−24072.
(44) Holmes, A.; et al. Highly Efficient Platinum-Free Photocatalytic Hydrogen Evolution From Low-cost Conjugated Polymer Nanoparticles. *Adv. Mater.* **2025**, *37*, 2507702.
(45) Kosco, J.; et al. Enhanced photocatalytic hydrogen evolution from organic semiconductor heterojunction nanoparticles. *Nat. Mater.* **2020**, *19*, 559−565.
(46) Dolan, A.; et al. Surfactant Effects on Hydrogen Evolution by Small-Molecule Nonfullerene Acceptor Nanoparticles. *ACS Appl. Nano Mater.* **2022**, *5*, 12154−12164.
(47) Kisch, H. On the Problem of Comparing Rates or Apparent Quantum Yields in Heterogeneous Photocatalysis. *Angew. Chem., Int. Ed.* **2010**, *49*, 9588−9589.
(48) Chen, Z.; et al. Accelerating materials development for photoelectrochemical hydrogen production: Standards for methods, definitions, and reporting protocols. *J. Mater. Res.* **2010**, *25*, 3−16.

https://doi.org/10.1021/acsenergylett.6c00531
ACS Energy Lett. 2026, 11, 4220−4229

(49) Costantino, F.; Kamat, P. V. Do *Sacrificial Donors* Donate H_2 in Photocatalysis? *ACS Energy Lett.* **2022**, *7*, 242−246.
(50) Huang, Y.; et al. Achieving a solar-to-chemical efficiency of 3.6% in ambient conditions by inhibiting interlayer charges transport. *Nat. Commun.* **2024**, *15*, 5406.
(51) Aitchison, C. M.; McCulloch, I. Organic Photovoltaic Materials for Solar Fuel Applications: A Perfect Match? *Chem. Mater.* **2024**, *36*, 1781−1792.
(52) Lin, W.-C.; et al. Effect of energy bandgap and sacrificial agents of cyclopentadithiophene-based polymers for enhanced photocatalytic hydrogen evolution. *Appl. Catal. B Environ.* **2021**, *298*, 120577.
(53) Li, Z.; et al. Three-Component Donor−π−Acceptor Covalent−Organic Frameworks for Boosting Photocatalytic Hydrogen Evolution. *J. Am. Chem. Soc.* **2023**, *145*, 8364−8374.
(54) Huang, T.-F.; et al. Flexible, nonfused sulfone functionalized polymer with enhanced active site access for photocatalytic sacrificial hydrogen evolution. *Sci. Adv.* **2025**, *11*, eadx1629.

https://doi.org/10.1021/acsenergylett.6c00531
ACS Energy Lett. 2026, 11, 4220−4229